Electronic Supplementary Material (ESI) for Green Chemistry.

Electronic Supporting Information (ESI)

Efficient and selective electrosynthesis of adiponitrile from electrohydrodimerization of acrylonitrile over the bismuth nanosheets modified electrode

Jia-Sheng Su[1+], Shih-Ching Huang[1+], Ming-Chi Tsai[1], Chia-Hui Yen[1], Chia-Yu Lin[1,2,3]*

[1]*Department of Chemical Engineering, National Cheng Kung University, Tainan City 70101, Taiwan*

[2]*Hierarchical Green-Energy Materials (Hi-GEM) Research Center, National Cheng Kung University, Tainan 70101, Taiwan.*

[3]*Program on Key Materials & Program on Smart and Sustainable Manufacturing, Academy of Innovative Semiconductor and Sustainable Manufacturing, National Cheng Kung University, Tainan, 70101 Taiwan*

+ These authors contributed equally.

* Corresponding authors: cyl44@mail.ncku.edu.tw

Contents

Experimental

Chemicals and Materials. All the chemicals, including acrylonitrile (AN; 99%, Sigma-Aldrich), adiponitrile (ADN; 99%, Sigma-Aldrich), sodium phosphate dibasic (≥99%, Sigma-Aldrich), sodium phosphate monobasic (≥99%, Sigma-Aldrich), bismuth(III) nitrate pentahydrate (≥98%, Sigma-Aldrich), lead(II) nitrate (≥99%, Sigma-Aldrich), potassium iodide (≥99.5%, Sigma-Aldrich), p-benzoquinone (≥98%, Sigma-Aldrich), boric acid (≥99.5%, Sigma-Aldrich), hydrochloric acid (≥37%, Sigma-Aldrich), sodium hydroxide (≥98%, Sigma-Aldrich), nitric acid (≥65%, Sigma-Aldrich), phosphoric acid (85%, Sigma-Aldrich), propanenitrile (PN; 99%, Acros Organics), 1, 3, 6-tricyanohaxane (Trimer; >98%, TCI), dimethyl sulfoxide (99.8%, Scharlau), tetrabutylammonium phosphate monobasic (TBAP; 97%, Angene), acetone (≥99.5% for HPLC, TEDIA), were used as received from the commercial suppliers without further purification. De-ionized water (18.2 MΩ cm; DIW) was used throughout this work to prepare electrolyte solutions for electrode fabrication and electrochemical measurements.

Electrode preparation. All the catalytic materials were deposited onto the copper foil electrochemically using a CHI 760E potentiostat (CH Instruments, Inc., USA) connected with a customized three-electrode electrochemical cell with Ag/AgCl (sat'd KCl) reference electrode and Pt foil (1 cm × 4 cm) counter electrode.

The electrodeposition of bismuth thin film (Bi_{film}) was performed in the plating solution containing nitric acid (1.0 M) and bismuth nitrate (30 mM) at -5 mA cm^{-2} till a specific charge passage ($Q_{Bi\ film}$) has been reached.

The electrodeposition of lead nanorods (nanoPb) was carried out in the plating solution containing boric acid (0.1 M) and lead nitrate (0.1 M) at -20 mA cm^{-2} till the charge passage of -1.5 C cm^{-2} was reached. After the electrodeposition, the obtained nanoPb electrode was further subjected to the potential cycling between -0.69 V and -1.34 V vs. Ag/AgCl at a scan rate of 100 mV s^{-1} for 4 cycles in phosphate solution (0.5 M, pH 8) containing TBAP (30 mM).

The electrodeposition of bismuth nanosheets (nanoBi) consisted of two steps, including (i) the electrodeposition of BiOI nanosheets (nanoBiOI) in the plating solution containing bismuth nitrate (40 mM), potassium iodide (0.4 M), and *p*-benzoquinone (50 mM) at -0.1 V vs. Ag/AgCl for 4 min, and (ii) the electrochemical reduction of nanoBiOI in borate buffer (0.1 M, pH 9.2) at -1.94 V vs. Ag/AgCl for 30 min.

Physical characterization. The surface composition and the oxidation state of the metal species in the prepared electrodes were analyzed using X-ray photoelectron spectroscopy (XPS) with a PHI 5000 VersaProbe system (ULVAC-PHI, Chigasaki, Japan). To minimize the contribution of the residuals of the bulk AN molecule to the XPS signals, all the samples were thoroughly rinsed prior to the XPS analyses. The obtained XPS spectra were calibrated to the binding energy of the C 1s peak to 284.6 eV. The surface morphology of the prepared electrodes was characterized using a Hitachi SU-8010 scanning electron microscope (SEM) equipped with energy-dispersive X-ray spectroscopy (EDS). The loading amount of Pb species (N_{Pb}) and Bi species (N_{Bi}) in the prepared electrodes was quantified using a Horiba Jobin Yvon JY 2000−2 ICP optical emission spectrometer (ICP-OES). X-ray diffraction (XRD) analyses were performed using an Ultima IV (Rigaku Co., Japan) X-ray diffractometer. The molecular weight of the oligomer was analyzed using a gel permeation chromatography (GPC) system, equipped with three linear columns (Shodex GPC KF-803L, KF-804L, and KF-805L) and a RI detector (Viscotek VE 3580), with tetrahydrofuran as the solvent at a flow rate of 1.0 mL min^{-1}.

Electrochemical characterization. The electrocatalytic performance of the prepared electrodes towards the electrohydrodimerization of AN (*EHD*-AN) was characterized at room temperature in a customized H-cell or flow-type electrolyzer (**Scheme S1** and **Figure 6a**) that is connected to a CHI 760E potentiostat (CH Instruments, Inc., USA) or a Ivium-n-Stat workstation (Ivium Technologies B.V., Netherlands). The anodic and cathodic compartments of the H-cell and flow-type electrolyzer

were separated with a Neosepta ASE anion exchange membrane (ASTOM Corporation, Tokyo, Japan). The prepared electrodes (i.e., Bi_{film}, nanoPb, and nanoBi) were used as the working electrode and placed with Ag/AgCl (sat'd KCl) reference electrode in the cathodic compartment, whereas the Pt (H-cell) or nickel foam (flow-type electrolyzer) was used as the counter electrode and placed in the anodic compartment. The linear sweep voltammetry (LSV), recorded at a scan rate of 10 mV s^{-1}, and 2-h controlled-potential electrolysis (CPE) were performed in the de-aerated phosphate solution (0.5 M) containing AN and TBAP under the purge of N_2 gas (99.99%; Yun Shan Gas Co., Taiwan) with 95% IR compensation. The effects of electrolyte composition and pH were investigated and optimized in the H-cell. The composition of catholyte and anolyte are the same for the experiments performed using H-cell. The compositions of the catholyte and anolyte for the CCEs at -100 mA cm^{-2} in the flow-type electrolyte were different; the cathodic electrolyte was the phosphate solution (0.5 M, pH 8) containing AN (0.6 M) and TBAP (30 mM), whereas the anolyte electrolyte was the NaOH solution (1.0 M) containing AN (0.6 M). The flow rates of catholyte and anolyte for the CCEs at -100 mA cm^{-2} in the flow-type electrolyte were set at 212.5 sccm. Unless noted, the applied potentials were referenced to the reversible hydrogen electrode (RHE) by using Eq. 1:

$$E\ (V\ vs.\ RHE) = E\ (V\ vs.\ Ag/AgCl) + 0.197 + 0.059 \times pH \quad (1)$$

The amount of electrochemically available lead species (e-N_{Pb}) and bismuth species (e-N_{Bi}) in the nanoPb, Bi_{film}, and nanoBi electrodes were determined by firstly estimating the charge responsible for the Pb^0/Pb^{2+} and Bi^0/Bi^{3+} redox reactions via the integration of the area under the corresponding redox peaks in cyclic voltammograms, followed by converting the estimated charge into moles of lead and bismuth species using Faraday's law.

Product analysis. The main liquid products, *i.e.*, PN, ADN, and trimer, generated from the CPEs in different conditions were analyzed and quantified using GC-2010 Plus gas chromatography system (Shimadzu) equipped with a flame ionization detector and Rtx®-Volatiles column. The temperature of the GC oven was maintained at 80 °C for the first 7 min, and subsequently ramped, at 20 °C min^{-1}, to 250 °C and maintained at 250 °C for another 25 min. On the other hand, H_2 generated from CPEs was analyzed and quantified with an Agilent 7890A Series gas chromatography (GC) equipped with a thermal conductivity detector (TCD) and HP-PLOT Molesieve 19095P-MS6 column. The temperature of the GC oven holding the columns was kept at 40 °C for the first 8 min, and subsequently ramped, at a rate of 40 °C/min, 200 °C and maintained at 200 °C for another 6 min.

The amount of ADN (N_{ADN}), trimer (N_{trimer}), PN (N_{PN}), and H_2 (N_{H2}) were obtained by converting the measured GC signals with routinely updated calibration curves. The charge consumed ($Q_{product}$), average current density ($J_{product}$), and corresponding current efficiency ($CE_{product}$) for the formation of these four products were then determined, respectively, using Eq. 2, Eq. 3, and Eq. 4:

$$Q_{product} = N_{product} \times n \times F \quad \text{(product: ADN, trimer, PN, or } H_2\text{)} \quad (2)$$

$$J_{product} = \frac{Q_{product}}{t_{CPE}} \quad \text{(product: ADN, trimer, PN, or } H_2\text{)} \quad (3)$$

$$CE_{product} = \frac{Q_{product}}{Q_{total}} \times 100\% \quad \text{(product: ADN, trimer, PN, or } H_2\text{)} \quad (4)$$

where n is the number of electron transfer, F is the Faradaic constant (96,485 C mol^{-1}), t_{CPE} is the duration of CPE (i.e., 2 h), and Q_{total} is the total charge passed in each CPE. The n value of 2 was used for the determination of $Q_{product}$.

Overpotential, an important parameter describing the kinetics of *EHD*-AN at a specific electrode, was defined as the difference between the thermodynamically-determined reduction potential of *EHD*-AN (i.e., 0.67 V vs. RHE[1]) and the applied potential to drive the *EHD*-AN at a specific current density. The selectivity of the prepared electrodes towards the ADN production (S_{ADN}) was evaluated and determined by using the ratio of the charge used for the ADN production (Q_{ADN}) to that used for the electrochemical reductions involving the consumption of AN (Q_{AN}), including the hydrolysis of ADN and reductive oligomerization of AN, with the assumption that HER is the only one competing electrochemical reaction without the consumption of AN (Eq. 5).

$$S_{ADN}(\%) = \frac{Q_{ADN}}{Q_{AN}} \times 100\% = \frac{N_{ADN} \times 2F}{Q_{total} \times (1 - CE_{H_2})} \times 100\% = \frac{CE_{ADN}}{(1 - CE_{H_2})} \times 100\% \quad (5)$$

Note that a noticeable amount of AN volatilized during the N_2 purge, and the changes in the amount of AN were therefore not equal to the amount of AN actually consumed for *EHD*-AN. In other words, the correct determination of AN conversion and yield of ADNs is therefore not possible in our experimental set-up. The oligomer factor, used to evaluate the extent of oligomerization of AN radical anion ($AN^{\bullet -}$) with AN molecule to form ADN and trimer, was determined by Eq. 6:[2]

$$\text{Oligomer factor} = \frac{N_{ADN} + N_{trimer}}{N_{PN}} \quad (6)$$

Two kinds of turnover frequencies were used to evaluate the electrocatalytic activity of the prepared electrodes, including (i) TOF_{ADN}, defined as the ratio of the average ADN production rate (R_{ADN}) from each CPE experiment to the ICP-OES-quantified loading amount of metal species (N_m), and (ii) *e*-TOF_{ADN}, defined as the ratio of R_{ADN} to the electrochemically accessible amount of metal species (i.e., *e*-N_{Pb} and *e*-N_{Bi}). TOF_{ADN}, determined by using Eq. 7, was used to evaluate the overall electrocatalytic activity. On the other hand, *e*-TOF_{ADN}, determined by using Eq. 8, was used to access the intrinsic activity as the electrochemically accessible amount of metal species is the amount of metal species directly exposed to the electrolyte solution and responsible for the electrocatalysis.

$$TOF_{ADN} = \frac{R_{ADN}}{N_m} \quad \text{(m: Bi or Pb)} \quad (7)$$

$$e\text{-}TOF_{ADN} = \frac{R_{ADN}}{e\text{-}N_m} \quad \text{(m: Bi or Pb)} \quad (8)$$

Table S1 Comparison of the electrocatalytic performance of the developed bismuth-modified electrodes with those reported previously.[a]

Electrodes	Applied potential or current density	Electrolyte	CE_{ADN} (%)	S_{ADN} (%)	R_{ADN} (mmole $cm^{-2}h^{-1}$)	Ref.
Pb plate	-20 mA cm^{-2}	Aqueous solution containing TEAT[a] (1.0 M) and AN (0.1 M)	~80[b]	~ 75[b]	~0.30	3
Pb plate	-100 mA cm^{-2}	An emulsion of water, AN (25 wt%), buffer solution (10 wt%; pH 5) and TMAC[c] (3 wt%)	~75	N.A.[d]	~1.40	4
Rotating Pb rod	-200 mA cm^{-2}	Na_3PO_4 solution (pH 8) containing AN (0.56 M), ADN (0.28 M), EDTA (0.02 M) and TBAP[e] (0.02 M)	82	85	~3.06	5
Carbonized Pb-based MOF[f] modified Pb foil	-0.85 V vs. RHE	K_3PO_4 solution (pH 11) containing AN (0.6 M) and TBAP[e] (0.02 M)	67	~80	~0.08	6
Rotating Pb rod	-100 mA cm^{-2} (E_{op}[g]: -2.08 V vs. RHE)	Na_3PO_4 solution (pH 8) containing AN (0.56 M), ADN (0.28 M), EDTA (0.02 M) and TBAP[e] (0.01 M)	~80	~79	~1.47	7
Cd foil	-1.45 V vs. RHE	Na_3PO_4 solution (0.5 M, pH 9) containing AN (0.6 M), EDTA (0.03 M) and TBAH[h] (0.02 M)	83	83	~0.40	1
Cd foil	Pulse electrolysis (E_c[i]: -2.65 V vs. RHE; E_r[j]: 0.85 V vs. RHE)	Na_3PO_4 solution (0.5 M, pH 11) containing AN (0.6 M), EDTA (0.03 M) and TBAH[h] (0.02 M)	N.A.[d]	~94	~1.11	8
Cd foil	-20 mA cm^{-2} (E_{op}[g]: -1.05 V vs. RHE)	Cs_3PO_4 solution (0.5 M, pH 11) containing AN (0.6 M), EDTA (0.03 M) and TBAH[h] (0.02 M)	N.A.[d]	93	N.A.[d]	9
$Bi_{flim,op}$	-1.13 V vs. RHE	Na_3PO_4 solution (0.5 M, pH 8) containing AN (0.6 M) and TBAP[e] (0.03 M)	87.90 ± 0.31	87.90 ± 0.31	0.49 ± 0.01	This work
nanoBi	-1.13 V vs. RHE	Na_3PO_4 solution (0.5 M, pH 8) containing AN (0.6 M) and TBAP[e] (0.03 M)	81.10 ± 1.96	81.21 ± 1.96	1.28 ± 0.20	This work

[a]: tetraethylammonium p-toluenesulfonate; [b]: with ultrasonic irradiation; [c]: tetramethylammonium chloride; [d]: data not available; [e]: tetrabutylammonium phosphate; [f]: metal–organic framework; [g]: electrode potential at corresponding applied current density; [h]: tetrabutylammonium hydroxide; [i]: cathodic potential; [j]: resting potential.

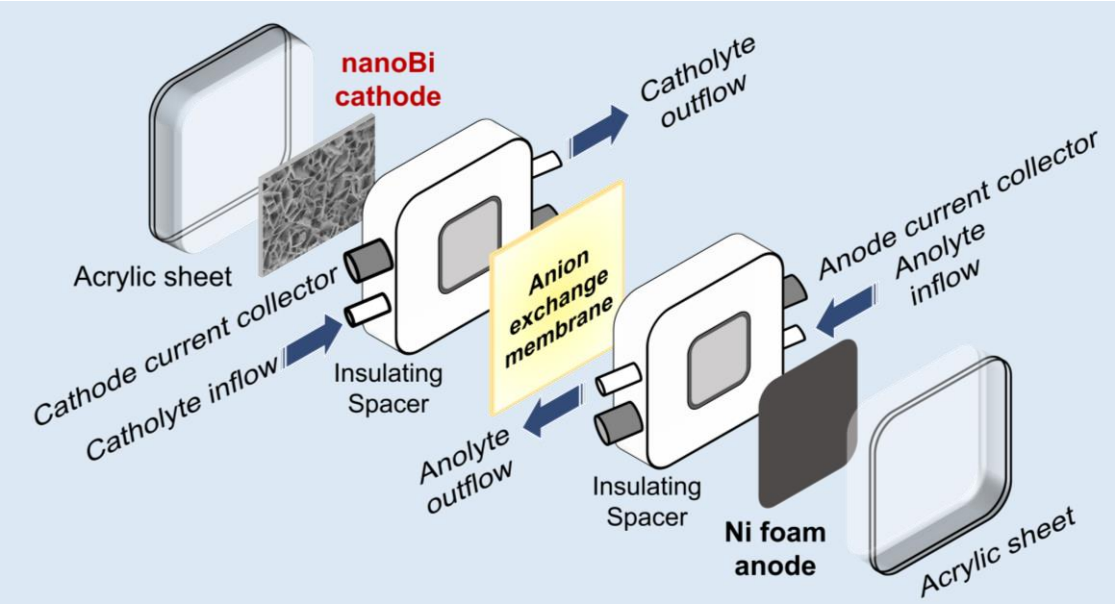

Scheme S1 Schematic illustration of the developed flow-electrolyzer..

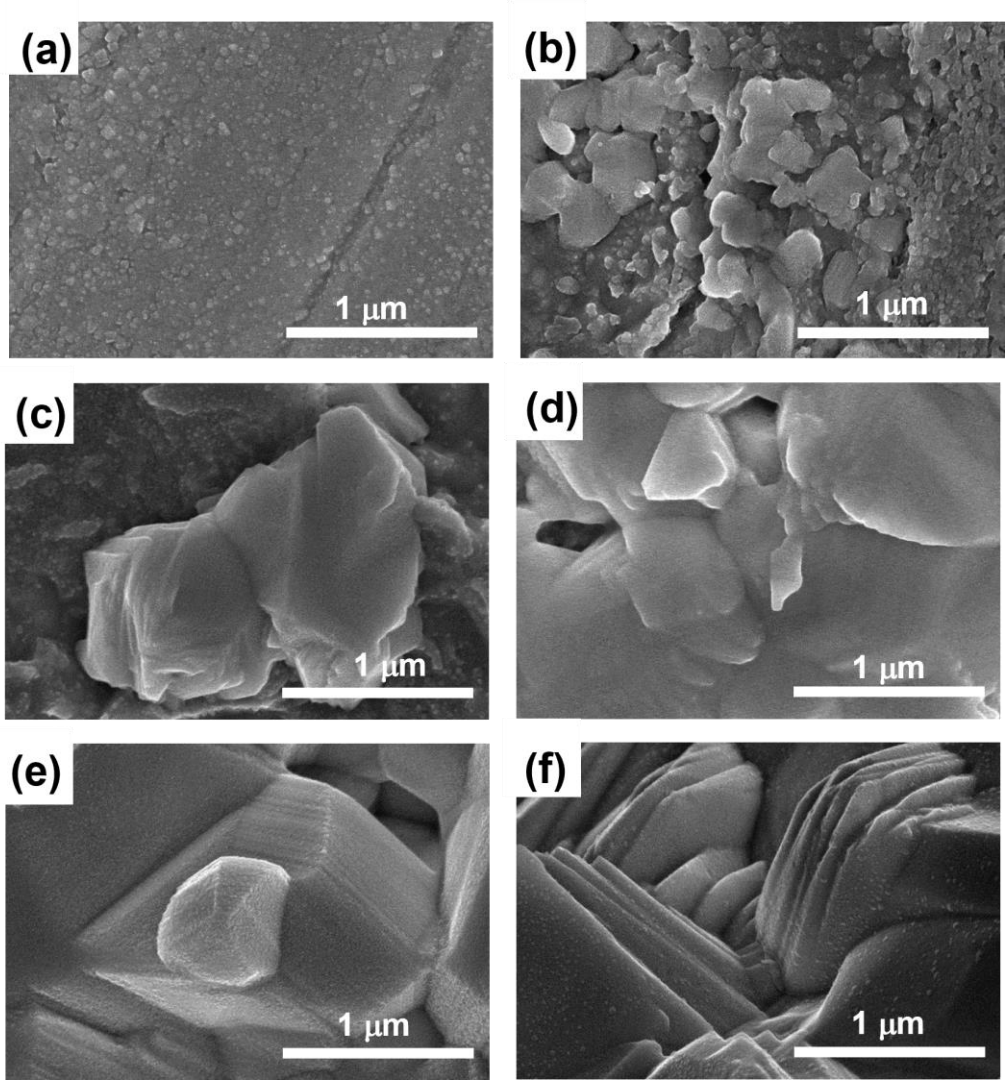

Figure S1 SEM images of (a) the bare copper substrate and (b-f) the Bi_{film} electrodes prepared with various $Q_{Bi\ film}$ (b: 0.025 C cm^{-2}; c: 0.25 C cm^{-2}; d: 0.5 C cm^{-2}; e: 1.0 C cm^{-2}; f: 1.5 C cm^{-2}).

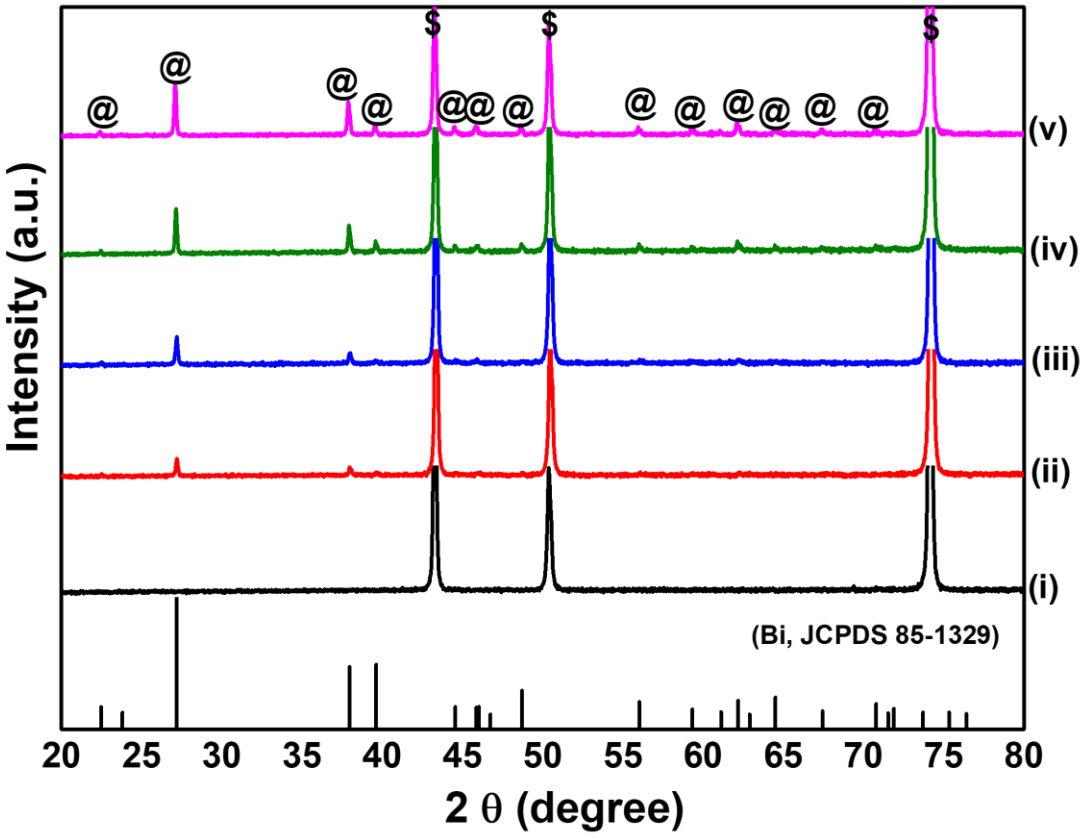

Figure S2 XRD patterns of the Bi_{film} electrodes prepared with various $Q_{Bi\ film}$ (i: 0.025 C cm^{-2}; ii: 0.25 C cm^{-2}; iii: 0.5 C cm^{-2}; iv: 1.0 C cm^{-2}; v: 1.5 C cm^{-2}). @ and $ are symbols standing for metallic bismuth (JCPDS 85-1329) and copper substrate, respectively.

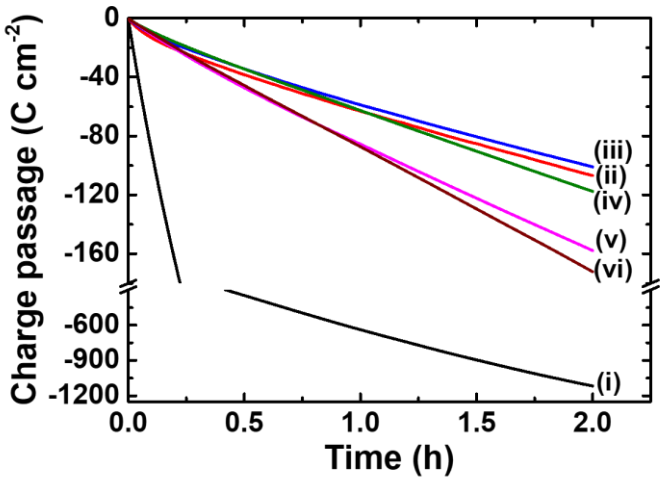

Figure S3 Charge transients obtained from the 2-h CPEs using (i) the bare copper substrate and the $Bi_{film,op}$ electrodes prepared with various $Q_{Bi\ film}$ (ii: 0.025 C cm^{-2}; iii: 0.25 C cm^{-2}; iv: 0.5 C cm^{-2}; v: 1.0 C cm^{-2}; vi: 1.5 C cm^{-2}) at -1.13 V in phosphate solution (0.5 M, pH 8) containing AN (0.6 M) and TBAP (20 mM).

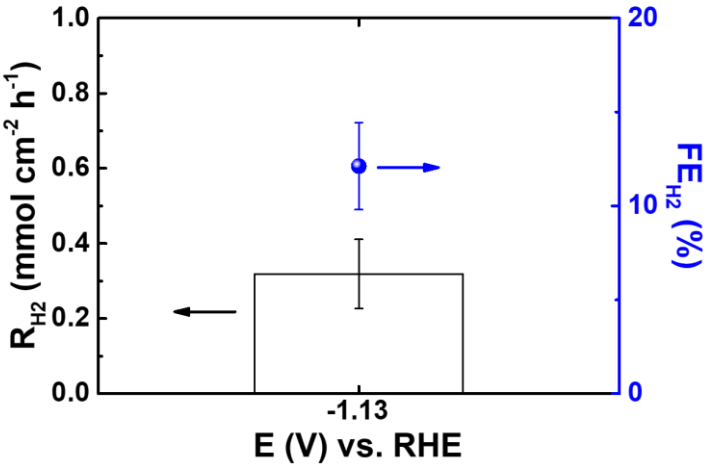

Figure S4 R_{H2} and FE_{H2} obtained from the 2-h CPEs of the bare copper foil at -1.13 V in phosphate solution (0.5 M, pH 8) containing AN (0.6 M) and TBAP (20mM).

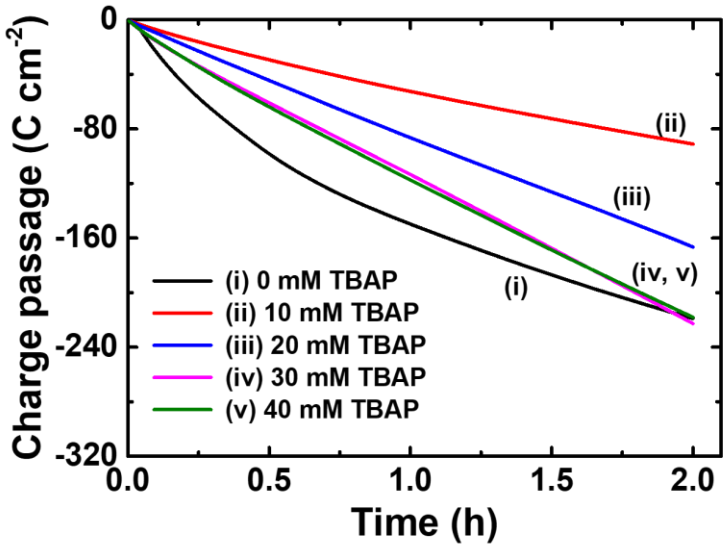

Figure S5 Charge transients obtained from the 2-h CPEs at -1.13 V using the $Bi_{film,op}$ electrode in phosphate solution (0.5 M, pH 8) containing AN (0.6 M) and TBAP of various concentrations.

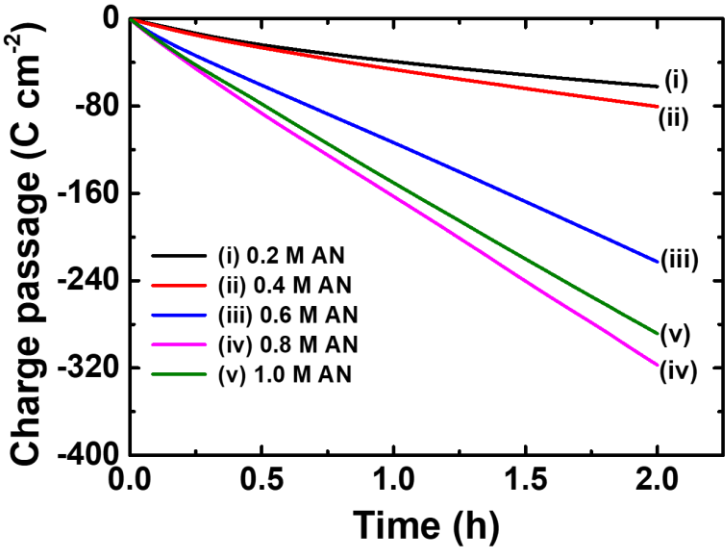

Figure S6 Charge transients obtained from the 2-h CPEs at -1.13 V using the $Bi_{film,op}$ electrode in phosphate solution (0.5 M, pH 8) containing TBAP (30 mM) and AN of various concentrations.

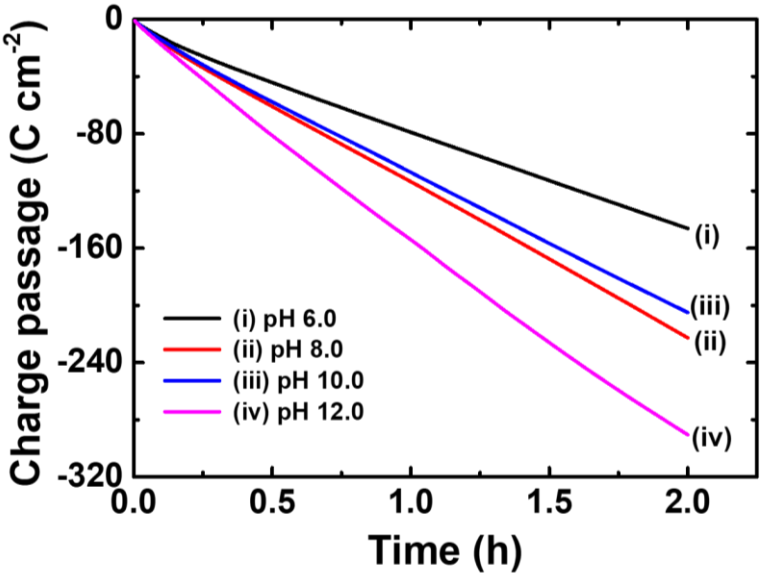

Figure S7 Charge transients obtained from the 2-h CPEs at -1.13 V using the $Bi_{film,op}$ electrode in phosphate solution (0.5 M, pH 6~12) containing AN (0.6 M) and TBAP (30 mM).

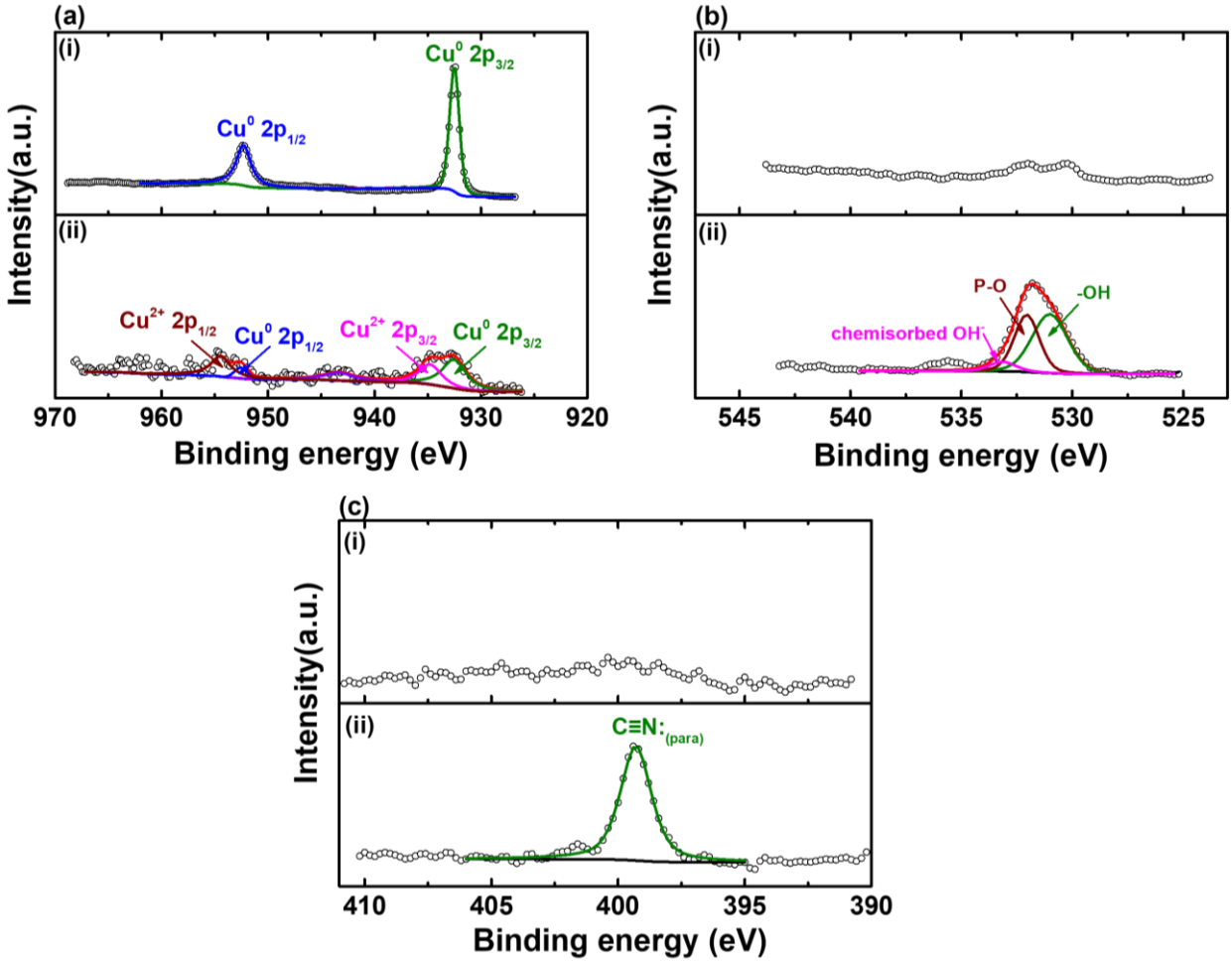

Figure S8 XPS spectra of the bare copper foil (i) before and (ii) after 2-h CPE at -1.13 V vs. RHE in in phosphate solution (0.5 M, pH 8) containing AN (0.6 M) and TBAP (30 mM). (a) Cu 2p region. (b) O 1s region. (c) N 1s region.

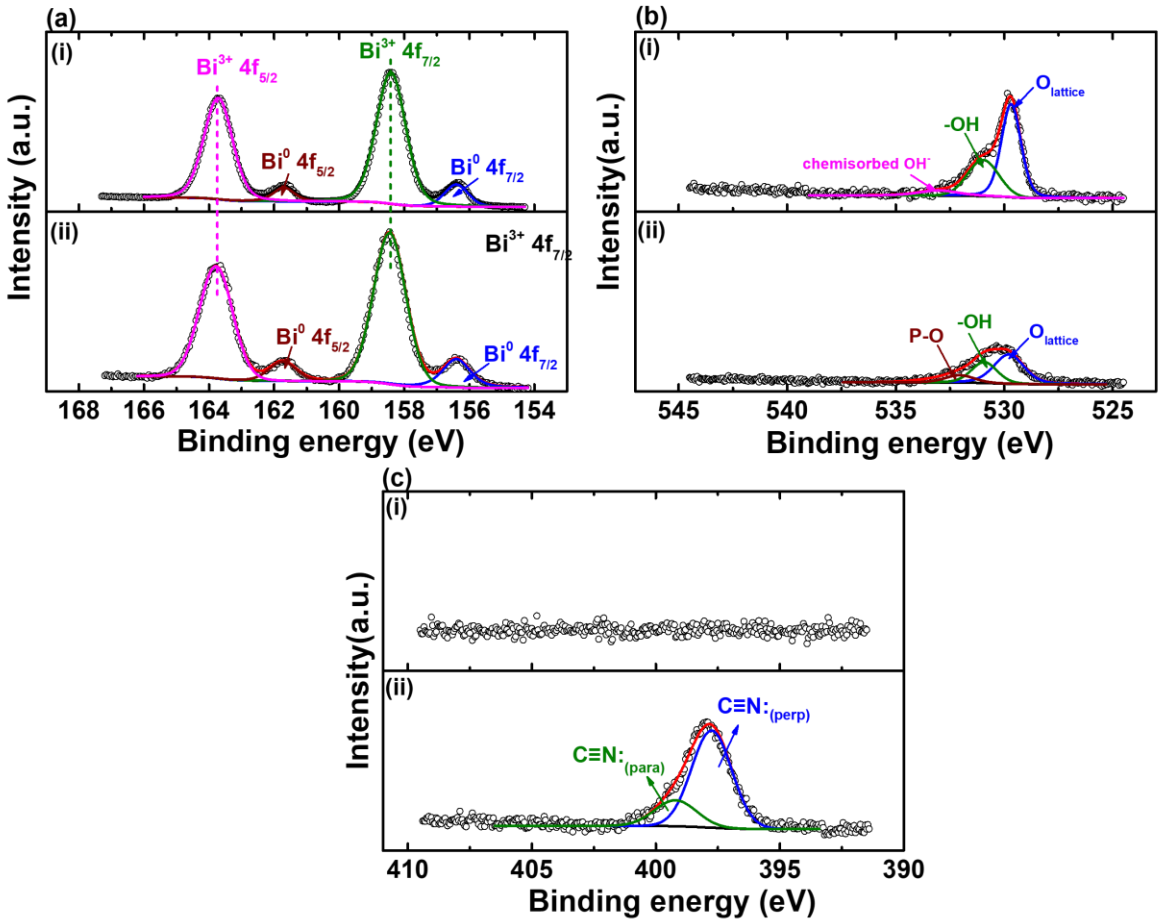

Figure S9 XPS spectra of the $Bi_{film,op}$ electrode (i) before and (ii) after 2-h CPE at -1.13 V vs. RHE in phosphate solution (0.5 M, pH 8) containing AN (0.6 M) and TBAP (30 mM). (a) Bi 4f region. (b) O 1s region. (c) N 1s region.

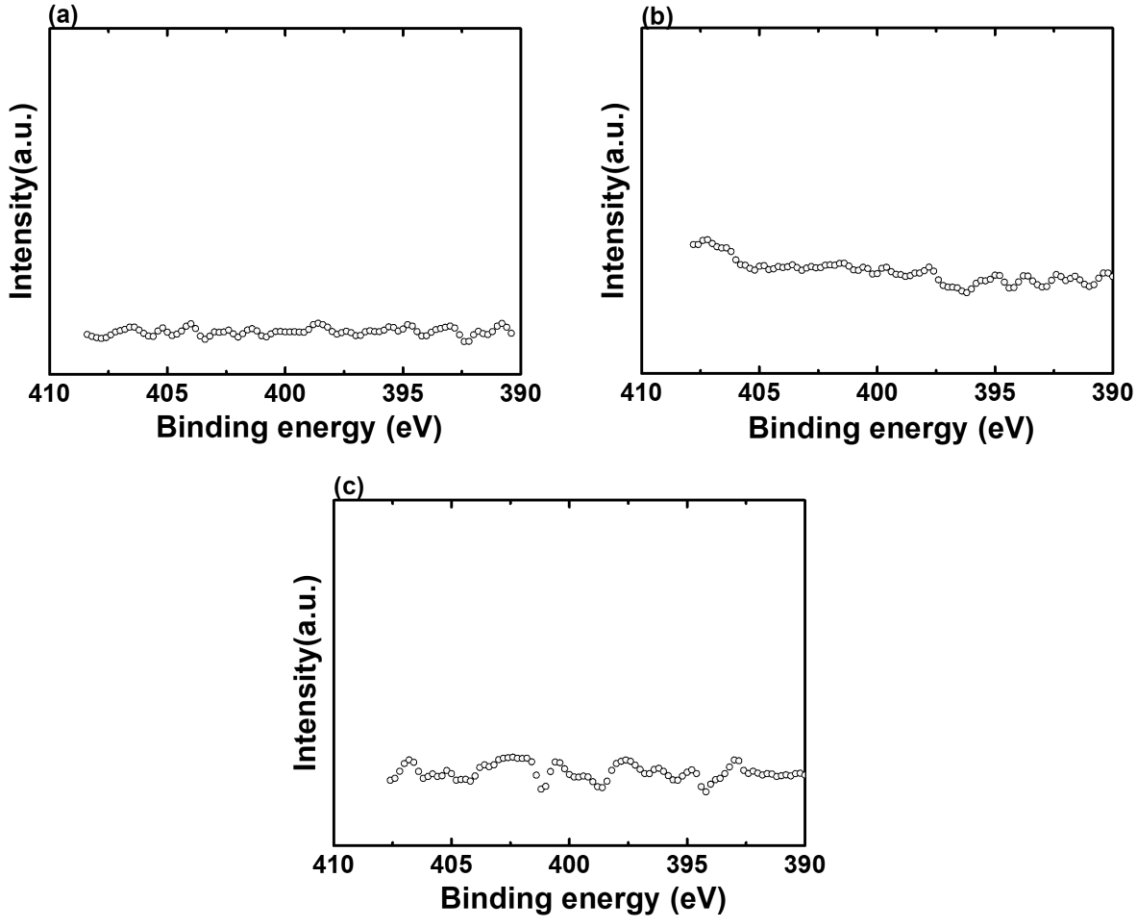

Figure S10 N 1s spectra of (a) the copper electrode, (b) the $Bi_{film,op}$ electrode, and (c) the nanoPb electrode after 2-h incubation in phosphate solution (0.5 M, pH 8) containing AN (0.6 M) and TBAP (30 mM) without applied any electricity.

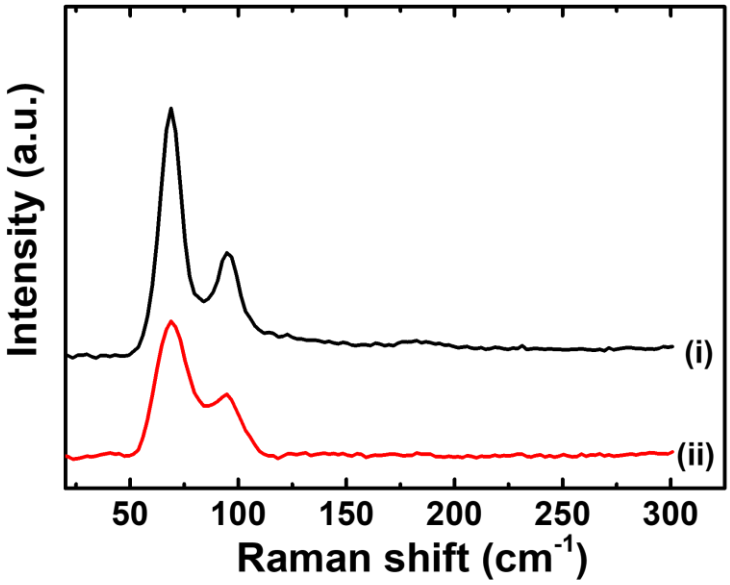

Figure S11 Raman spectra of (i) the as-prepared $Bi_{film,op}$ and (ii) the as-prepared nanoBi electrode.

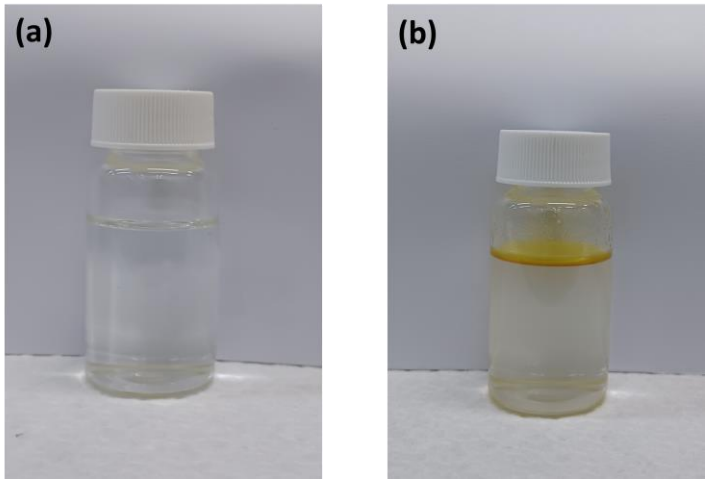

Figure S12 Digital photographs of the electrolyte solution (pH 8), consisting of phosphate (0.5 M), AN (1.0 M), and TBAP (30 mM), (a) before and (b) after 2-h CPE at -1.13 V vs. RHE.

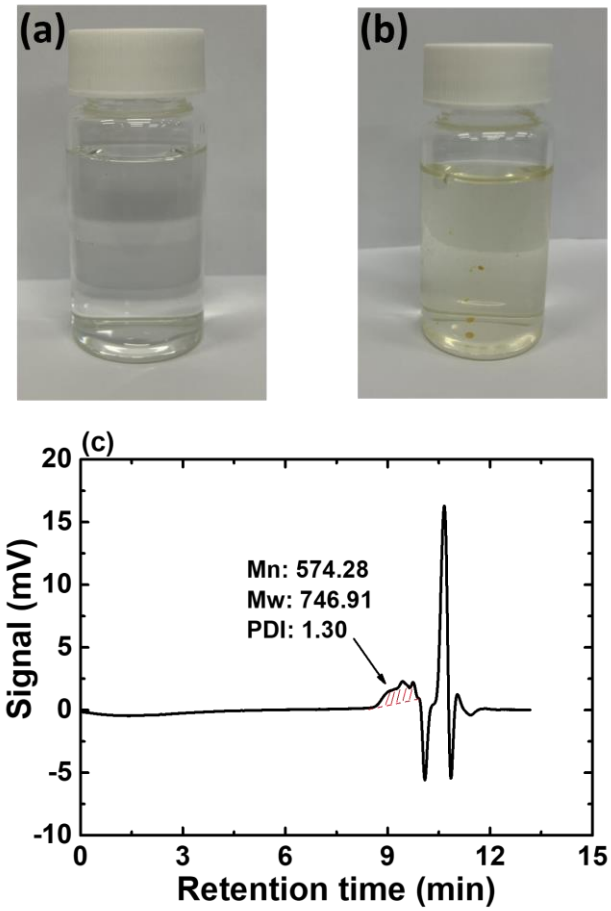

Figure S13 (a, b) Digital photographs of the electrolyte solution (pH 8), consisting of phosphate (0.5 M), AN (0.6 M), and TBAP (30 mM), before (a) and after (b) 2-h CPE at -1.23 V vs. RHE. (c) GPC chromatogram of the isolated electrolyte solution after 2-h CPE at -1.23 V vs. RHE.

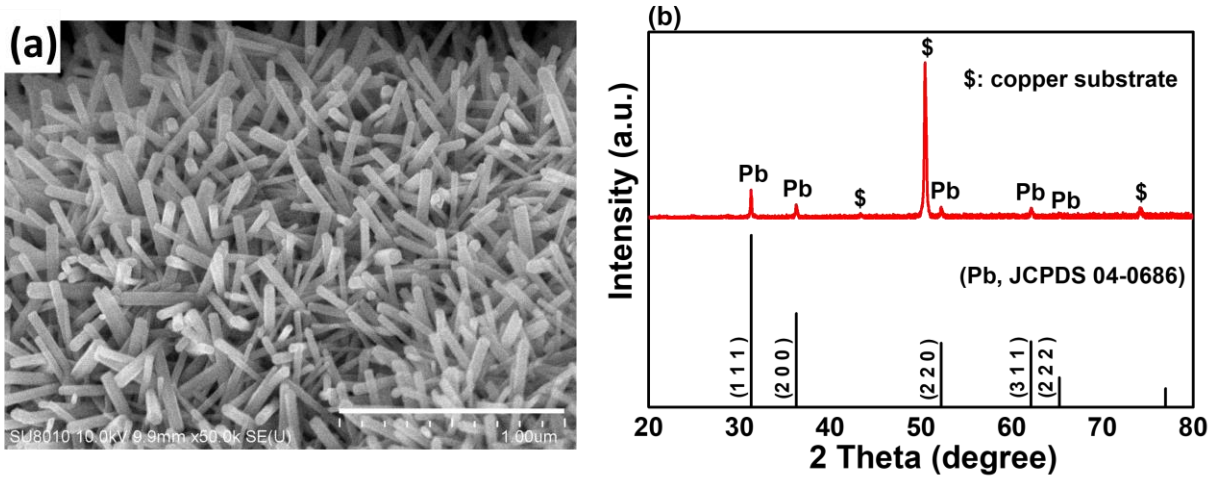

Figure S14 (a) SEM image and (b) XRD of the prepared nanoPb electrode.

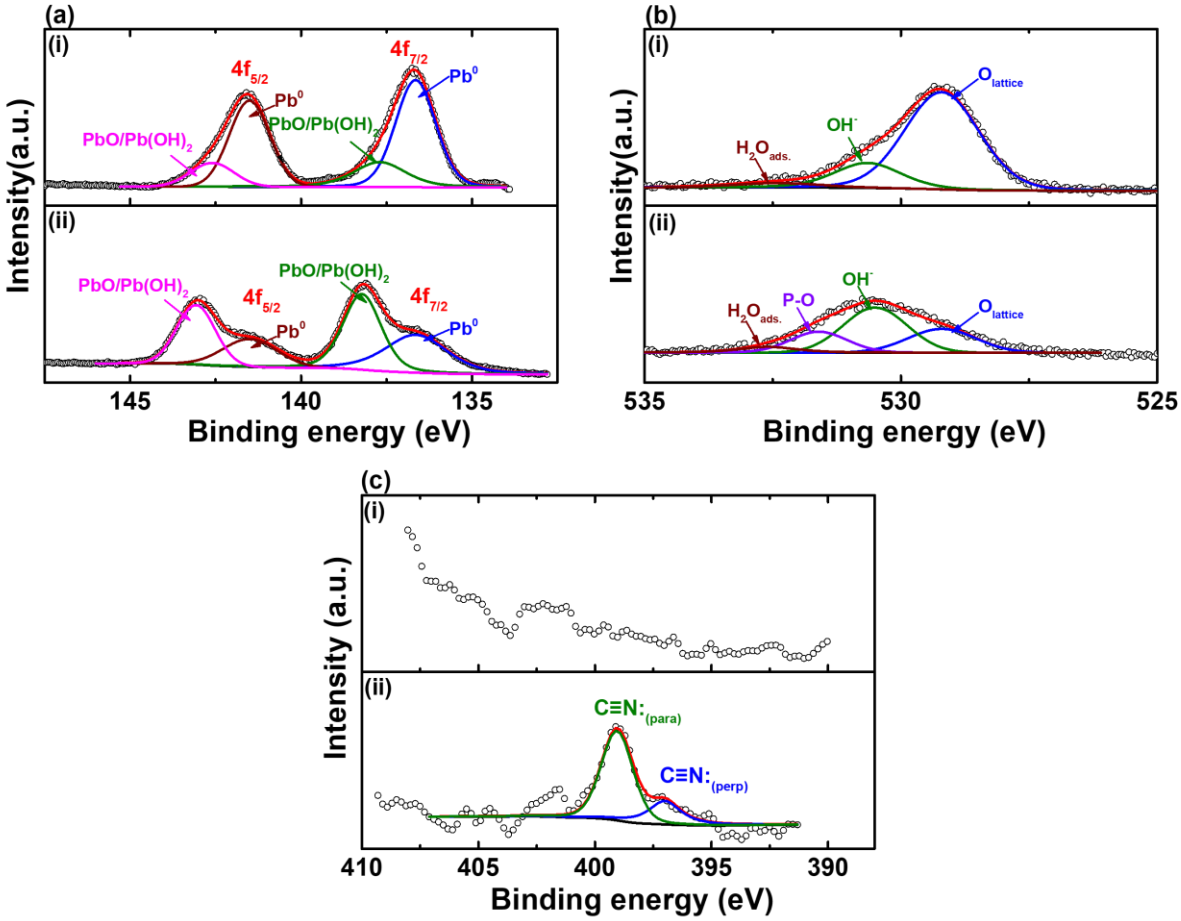

Figure S15 XPS spectra of the nanoPb electrode (i) before and (ii) after 2-h CPE at -1.13 V vs. RHE in phosphate solution (0.5 M, pH 8) containing AN (0.6 M) and TBAP (30 mM). (a) Pb 4f region. (b) O 1s region. (c) N 1s region.

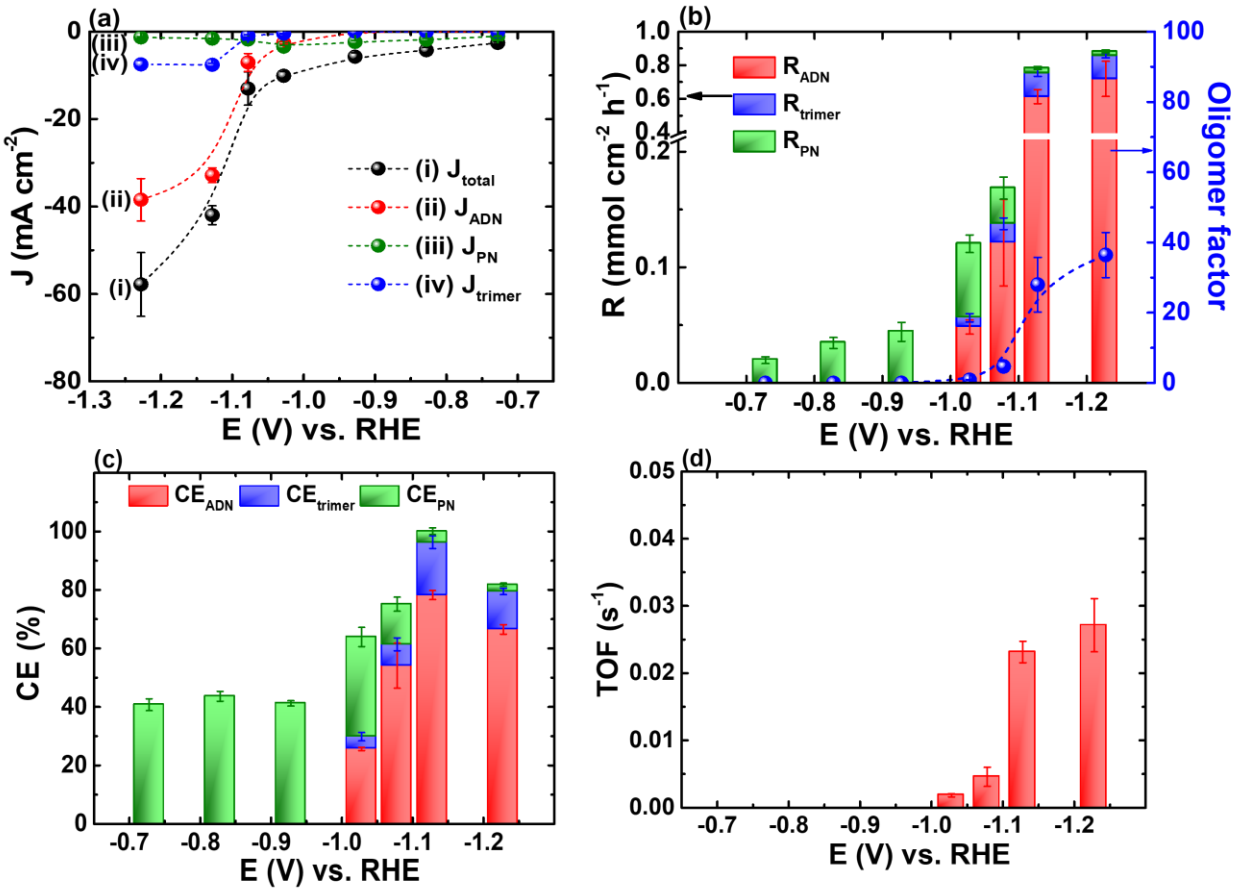

Figure S16 (a) J (i: J_{total}; ii: J_{ADN}; iii: J_{PN}; iv: J_{trimer}), (b) generation rate (R) of products, (c) CEs of the generated products, and (d) TOF_{ADN} obtained from 2-h CPEs using the nanoPb electrode at various applied potentials in phosphate solution (0.5 M, pH 8) containing AN (0.6 M) and TBAP (30 mM).

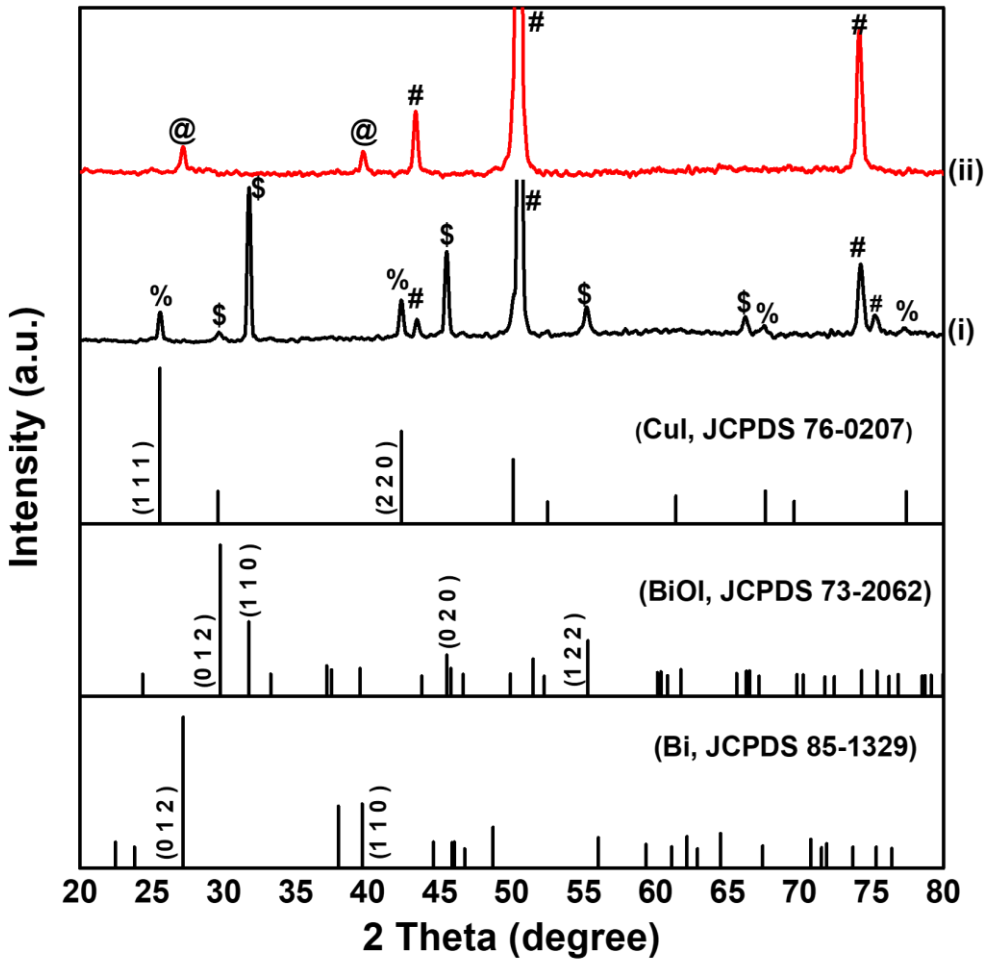

Figure S17 XRD of (i) the nanoBiOI electrode and (ii) the nanoBi electrode. Diffraction peaks noted with @, #, %, and $ are assigned to metallic bismuth, copper substrate, CuI, and BiOI, respectively.

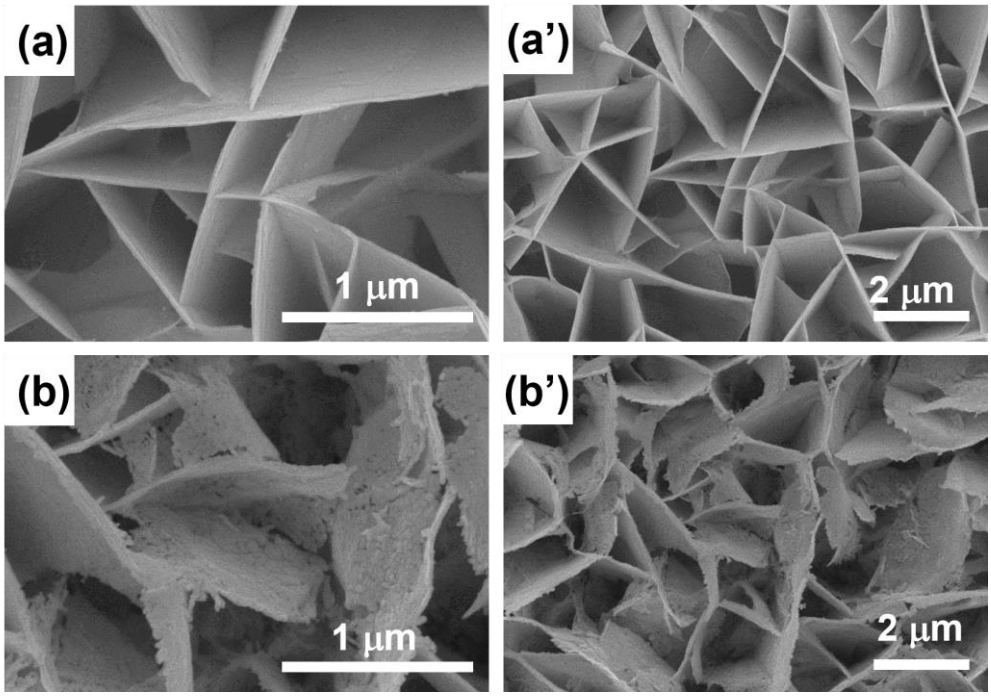

Figure S18 SEM images at different magnifications of (a, a') the nanoBiOI electrode and (b, b') the nanoBi electrode.

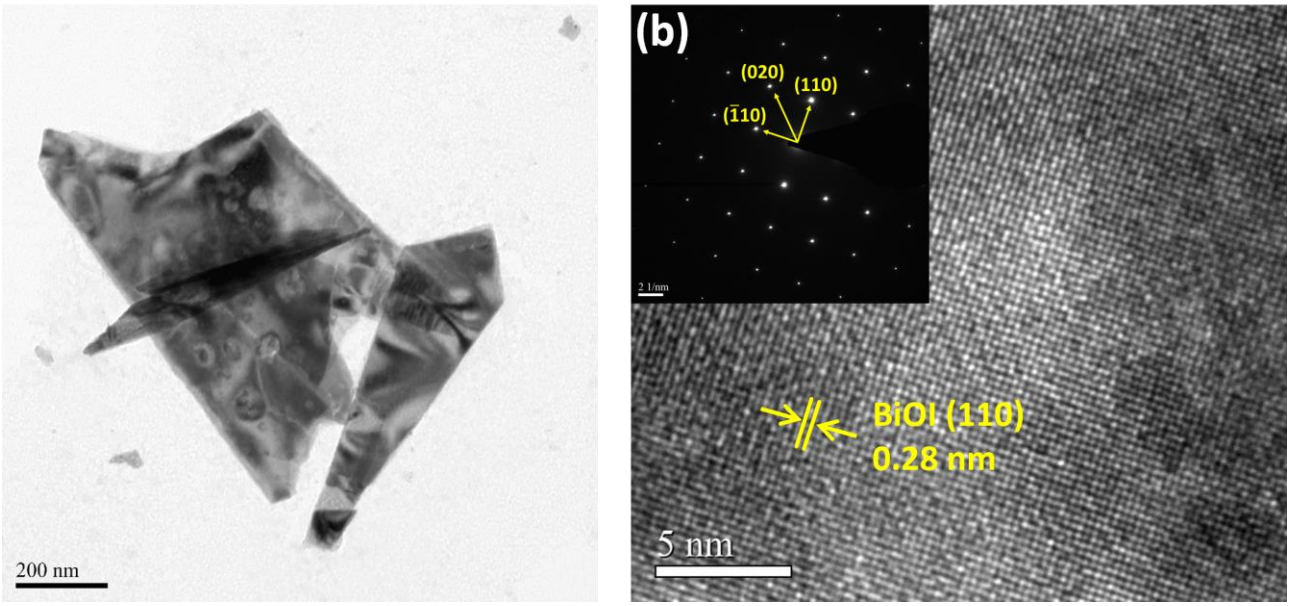

Figure S19 (a) TEM image and (b) HRTEM image and SAED pattern (inset) of the nanoBiOI electrode.

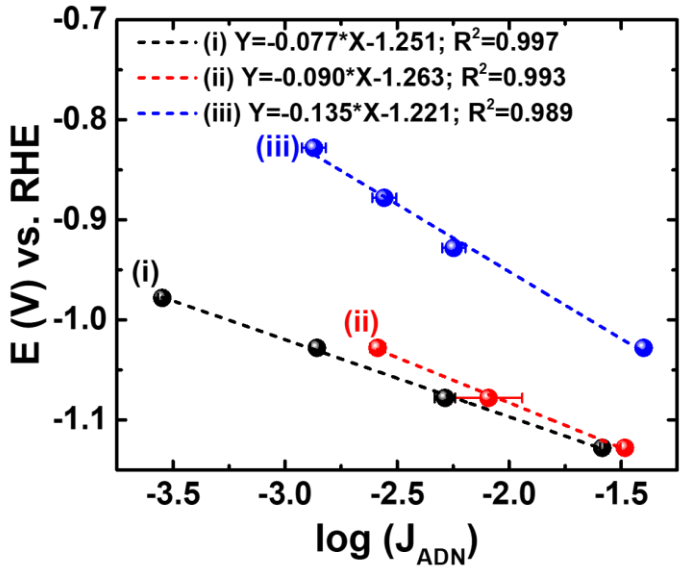

Figure S20 Tafel plots of (i) the $Bi_{flim,op}$ electrode, (ii) the nanoPb electrode, and (iii) the nanoBi electrode obtained from the 2-h CPEs in phosphate solution (0.5 M, pH 8) containing AN (0.6 M) and TBAP (30 mM).

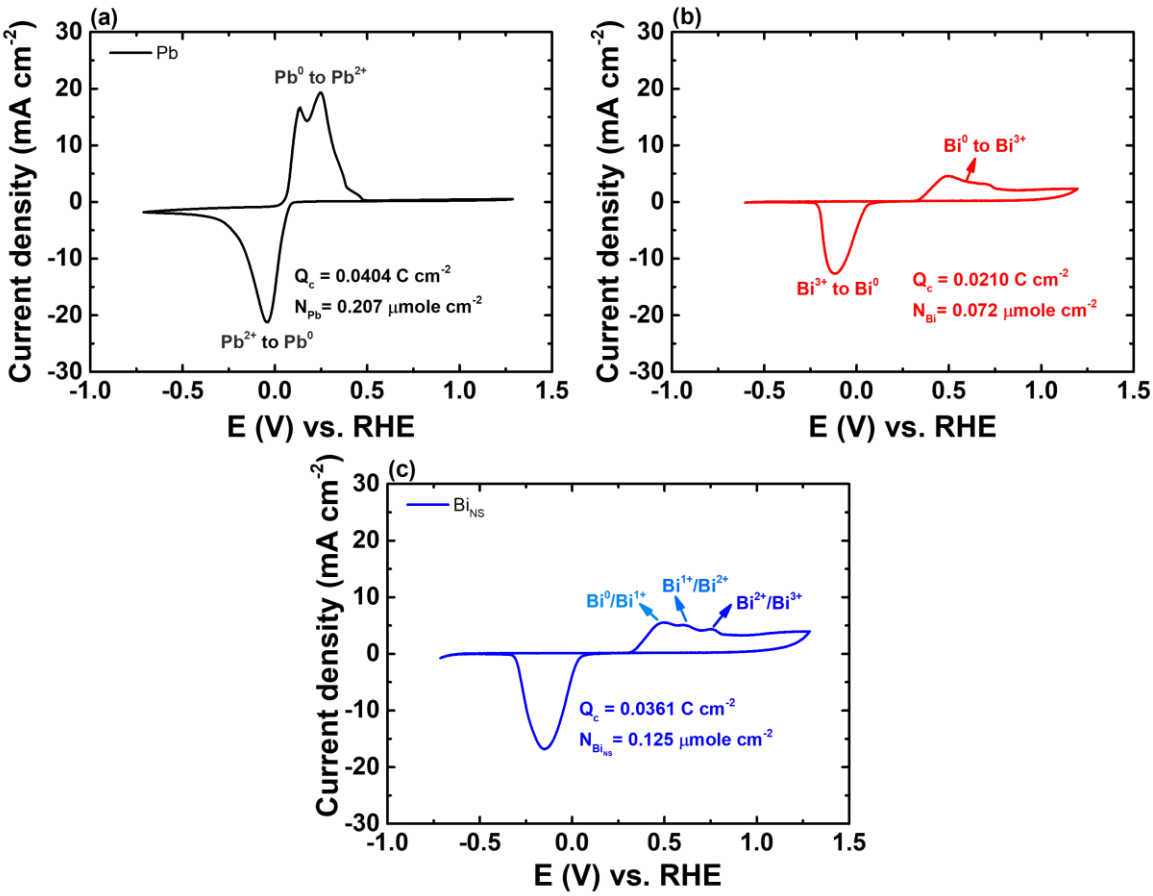

Figure S21 CVs, at a scan rate of 100 mV s^{-1}, of (i) the nanoPb electrode, (ii) the $Bi_{flim,op}$ electrode, and (iii) the nanoBi electrode obtained sodium bicarbonate (0.5 M).

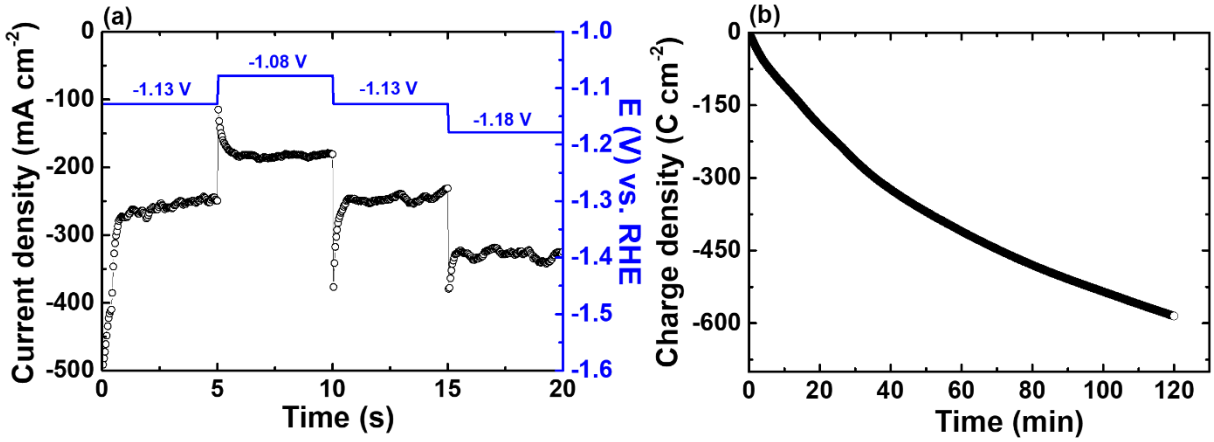

Figure S22 (a) Current response to the applied potential waveform recorded in the first cycle, and (b) charge transient recorded during the 2-h CPE under fluctuated applied potentials in phosphate solution (0.5 M, pH 8) containing AN (0.6 M) and TBAP (30 mM).

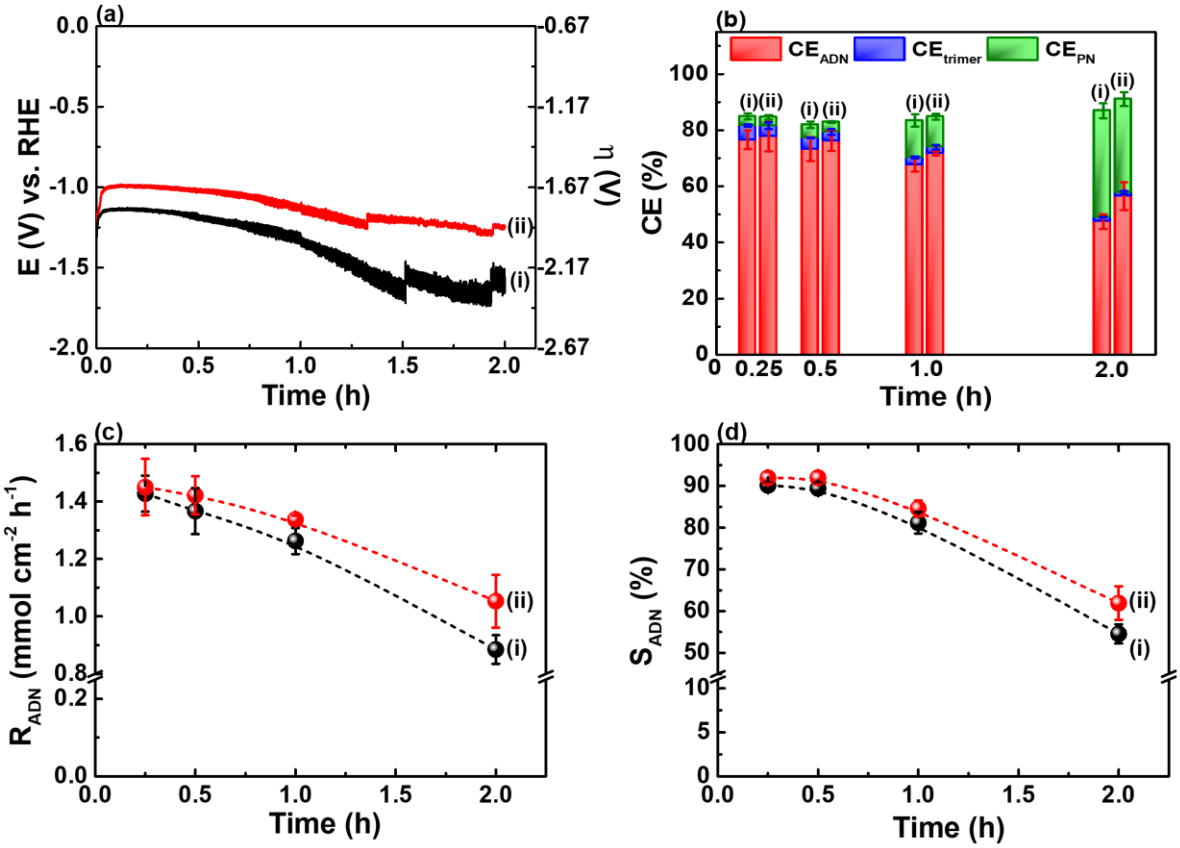

Figure S23 (a) Typical potential/η transient, (b) CEs of the generated products, (c) R_{ADN}, and (d) S_{ADN} recorded during the electrolysis using the Pb foil (i) and nanoBi electrode (ii) at -100 mA cm^{-2} in phosphate solution (0.5 M, pH 8) containing AN (0.6 M) and TBAP (30 mM).

References:

1. D. E. Blanco, A. Z. Dookhith and M. A. Modestino, *React. Chem. Eng.*, 2019, **4**, 8-16.
2. B. Y. Li, W. F. Huang and M. C. Yang, *J. Taiwan Inst. Chem. Eng.*, 2020, **115**, 13-19.
3. M. Atobe, M. Sasahira and T. Nonaka, *Ultrason. Sonochem.*, 2000, **7**, 103-107.
4. F. Karimi, S. N. Ashrafizadeh and F. Mohammadi, *Chem. Eng. J.*, 2012, **183**, 402-407.
5. B.-Y. Li, W.-F. Huang and M.-C. Yang, *J. Taiwan Inst. Chem. Eng.*, 2020, **115**, 13-19.
6. Y.-C. Wang, J.-H. Yen, C.-W. Huang, T.-E. Chang, Y.-L. Chen, Y.-H. Chen, C.-Y. Lin and C.-W. Kung, *ACS Appl. Mater. Interfaces*, 2022, **14**, 35534-35544.
7. W.-F. Huang and M.-C. Yang, *Ind. Eng. Chem. Res.*, 2021, **60**, 13180-13190.
8. D. E. Blanco, B. Lee and M. A. Modestino, *Proc. Natl. Acad. Sci. U.S.A.*, 2019, **116**, 17683-17689.
9. D. E. Blanco, R. Atwi, S. Sethuraman, A. Lasri, J. Morales, N. N. Rajput and M. A. Modestino, *J. Electrochem. Soc.*, 2020, **167**, 155526.